Theoretical and Applied Climatology (2025) 156:169
https://doi.org/10.1007/s00704-025-05388-0

RESEARCH

Comprehensive evaluation of satellite precipitation products over sparsely gauged river basin in Nigeria

Habeeb Oladimeji Ganiyu[1,2] · Faridah Othman[1] · Wan Zurina Wan Jaafar[1] · Cia Yik Ng[1]

Received: 29 August 2024 / Accepted: 30 January 2025
© The Author(s), under exclusive licence to Springer-Verlag GmbH Austria, part of Springer Nature 2025

Abstract
The study evaluated GPM-IMERG07, CHIRPS2.0, CPC-CMORPH, and PERSIANN-CDR against ground observations of rainfall for five gauging stations over 10 years (2013–2022) in the Niger Central Hydrological Area, Nigeria. This area is prone to severe annual floods, which lead to devastating downstream effects. The lack of high-density and evenly distributed rain gauge stations has hindered effective research on mitigating flood impacts, necessitating alternative rainfall data sources. Satellite precipitation products (SPPs) are used globally because of their high temporal and spatial resolution, free accessibility, and extensive coverage. However, these products have inherent biases and require comprehensive evaluation. The study employed scatter plots and descriptive statistics for daily and monthly comparisons. Daily SPPs were further analyzed using categorical statistics and a four-component error decomposition method. The findings revealed a higher correlation and greater errors at the monthly temporal resolution than at the daily resolution. PERSIANN-CDR performed better (daily and monthly) with a slightly higher median correlation (0.33 and 0.86), RMSE (9.66 mm and 57.59 mm), and Bias (-0.13 and 4.02). Furthermore, it demonstrated exceptional rainfall detection probability (POD = 85%) and minimal miss bias (MB = 119.2 mm/day) compared to other SPPs. Therefore, the high performance of PERSIANN-CDR in most statistical indices validates its suitability for the study area. Nonetheless, SPPs exhibited high bias values above the perfect value of zero (0). Thus, it is recommended that algorithm developers reduce these biases to improve the suitability of SPPs. End users should also consider bias correction or data merging to enhance the accuracy of the hydrological simulations.

1 Introduction

Rainfall is a crucial component of the hydrological cycle that significantly affects the environment, including water resource management, agriculture, climate change studies, and flood hazard management (Adenodi et al. 2016). These applications require quality rainfall data from densely and evenly distributed rain gauge stations (Seyam and Othman 2015). Conventionally, ground observations are the most accurate means of rainfall measurements. However, their coverage is often limited and sparsely distributed in developing and mountainous regions, where the available gauging stations are insufficient to meet the requirements of the World Meteorological Organization (WMO) (Adenodi et al. 2016). This is mainly due to rain gauge network deployment challenges, including inaccessibility on steep remote slopes, financial constraints in developing areas, insufficient maintenance reducing efficiency, and extreme weather conditions damaging the gauges (Suri and Azad 2024). To overcome these limitations, satellite precipitation products (SPPs) have been developed to provide alternative rainfall sources with different temporal and spatial resolutions (Goshime et al. 2019; Worqlul et al. 2017). These products leverage advanced algorithms and multiple satellite datasets to estimate global precipitation based on infrared radiation where infrared sensors on geostationary satellites infer precipitation from the tops of clouds establishing a correlation between the temperatures and ground-level precipitation probability, microwave radiation which is predicated

✉ Faridah Othman
faridahothman@um.edu.my

✉ Wan Zurina Wan Jaafar
wzurina@um.edu.my

Habeeb Oladimeji Ganiyu
oladimejihabeeb88@gmail.com

Cia Yik Ng
ng.ciayik@gmail.com

[1] Department of Civil Engineering, Universiti Malaya, 50603 Kuala Lumpur, Malaysia

[2] Department of Civil Engineering, Kwara State University, 241104 Malete, Nigeria

Published online: 20 February 2025

on the relationship between surface precipitation and low-frequency microwave emissions from raindrops, as well as high-frequency microwave scattering from ice, combination of the two (Moges et al. 2022), and machine learning such as artificial neural network algorithm to calculate the quantity of rainfall from satellite longwave infrared imagery (Vu et al. 2018; Yazdandoost et al. 2020). The recent advancements in satellite data have increased interest in satellite rainfall monitoring, which offers benefits such as extensive continuous coverage and high temporal and spatial resolutions for various hydrological studies (Min et al. 2020).

The most commonly used SPPs in limited and sparse data regions include Climate Hazards Group InfraRed Precipitation with Station data (Funk et al. 2015), CPC Morphing Technique (CMORPH; Joyce et al. 2004), Integrated Multi-Satellite Retrievals for Global Precipitation Measurement (IMERG; Huffman et al. 2019), Precipitation Estimation from Remotely Sensed Information using Artificial Neural Networks (PERSIANN; Hsu et al. 1997), Tropical Rainfall Measuring Mission (TRMM) multi-satellite precipitation analysis (TMPA; Huffman et al. 2007), and Tropical Applications of Meteorology using SATellite (TAMSAT; Maidment et al. 2017). Precipitation rates are estimated by calibrating either visible/infrared (VIS/IR), or microwave (MW), measurements, with ground observations (Gebregiorgis et al. 2018; Yong et al. 2016). These products have been used for streamflow simulations in Brazil (Almagro et al. 2021), China (Khan et al. 2022; Peng et al. 2021), Ethiopia (Kabite Wedajo et al. 2021; Worqlul et al. 2017), Ghana (Adjei et al. 2015), Kenya (Le and Pricope 2017), Pakistan (Usman et al. 2022), and Thailand (Gunathilake et al. 2020) among other data-scarce regions. Studies have revealed that SPP performance varies across regions. This is because of sampling errors, data sources, precipitation measurement techniques (Hussain et al. 2017a, b; Yuan et al. 2017), climatic and geographical conditions, and terrain variations (Chen et al. 2014; Yong et al. 2016).

The study area, the Niger Central Hydrological Area (NCHA), located in the low-lying areas of the Niger River Basin, has experienced severe annual floods due to increased river water levels and discharge. These flood events have destructive impacts, particularly on the downstream of the basin. This constitutes a major threat to the country's efforts to achieve global sustainable development goals that target environmental and human development by 2030 (NIHSA 2022). Therefore, it is pertinent to simulate streamflow to develop a flood hazard map for flood mitigation. The hydrological simulation of an accurate streamflow requires a high density and an even distribution of rain gauge stations. Unfortunately, Nigeria has 87 existing and operating rain gauge stations covering a land area of approximately 923,300 km². This translates to 10,600 km^2 per gauge station. Conversely, achieving optimal coverage and meeting the WMO requirements for Tropical, Mediterranean, and Temperate zones would require a minimum of 1057 rain gauges (Ngene and Obianigwe 2022). In addition, researchers are faced with bureaucracy challenges and cost implications in acquiring observed rainfall data, limiting the number of studies on streamflow simulation in Nigeria's hydrological basins. Therefore, alternative sources of precipitation information such as SPPs are required. Few studies have applied SPPs to various hydrological simulations in Nigerian basins. These include precipitation forecasts (Yue et al. 2022), hydropower potential assessment (Fasipe and Izinyon 2021), assessment of flood events (Adedeji et al. 2021), and flood forecasting in the Niger-Benue Basin (Haile et al. 2016).

However, it is crucial to evaluate the suitability of SPPs before applying them to various hydrological studies because of their inherent biases. Few studies have assessed the accuracy of SPPs against ground observations in Nigeria. Salami and Fenta (2022) evaluated eight SPPs at daily, monthly, seasonal, and annual temporal resolutions. The results revealed the high performance of GPCC, CHIRPS, TAMSAT, CRU-TS, and GPM-IMERG. Akinyemi et al. (2020) validated TRMM, CHIRPS, and REF2.0 against ground observations at a monthly temporal resolution over six gauging stations in southwestern Nigeria. The results showed that TRMM and CHIRPS had a good relationship with the ground observations at most gauge locations. Nwachukwu et al. (2020) evaluated SPPs at eleven gauging stations and revealed the reliability of MSWEP2.2 and CHIRPS2.0. Ogbu et al. (2020) assessed the accuracy of CHIRPS, PERSIANN, and TAMSAT against ground observations at seasonal and annual temporal resolutions at 24 gauging stations in Guinea, Savannah, and Sahel regions. The statistical evaluation results showed the accuracy of CHIRPS over other SPPs in all climatic zones. Similarly, a study conducted with the coverage of 18 gauging stations in the Sahelian zone of Nigeria at daily, decadal, seasonal, and annual temporal resolutions demonstrated the high performance of CHIRPS (Usman et al. 2018). CHIRPS and TRMM (GPM-IMERG) have been consistently used and demonstrate good performance in Nigeria. This follows Dinku et al. (2018), who concluded that CHIRPS is the most accurate product in Africa, whereas Poméon et al. (2017) discovered that CMORPH and PERSIANN-CDR products are the best in West Africa. The evaluation of these SPPs in Nigeria is not comprehensive enough to determine their suitability, as they fail to measure the detectability of rainfall events and the quantity of error components in the SPPs. Therefore, this study comprehensively evaluated the suitability of CHIRPS2.0, CPC-CMORPH, PERSIANN-CDR, and the recently released GPM-IMERG final version 7 (GPM-IMERG07) against ground observations in the study area using categorical statistics and bias error decomposition, in

addition to the conventional approach. Categorical statistics identify the presence of rainfall and no rainfall (Qin et al. 2014), whereas bias error decomposition quantifies the individual error components in SPPs using the four-component error decomposition (4CED) developed by Zhang et al. (2021). 4CED includes hit positive bias (HPB), hit negative bias (HNB), false bias, and miss bias (MB). Understanding 4CED will enable developers to improve SPPs retrieval algorithms.

2 Methodology

2.1 Description of the study area

The Niger River has a basin area of 2,117,700 km^2 (Yue et al. 2022), making it the ninth largest river basin. The climate in this region is classified as tropical rainy and dry according to Köppen climate classification, with an average annual rainfall of 1159 mm, a temperature of 27.7°C, and a relative humidity of 60%. In Nigeria, there are eight (8) main hydrological areas which include Niger North, Niger Central, Upper Benue, Lower Benue, Niger South, Western Lithoral, Eastern Lithoral, and Chad Basin. The study area, Niger Central Hydrological Area (NCHA), covers Niger, Kwara, Kaduna, the Federal Capital Territory (FCT), Ekiti, and parts of Kogi States (NIHSA 2022), while the main rivers in the hydrological area include Niger, Kaduna, Kampe, Usuma, Gurara, and Awun. The NCHA is situated in the transitional zone between a semi-arid climate in the north and a sub-humid climate in the south, which is influenced by the seasonal movement of the intertropical convergence zone. This results in both the wet and dry seasons. The wet season typically spans from April to October, and the dry season extends from November to March (Otache et al. 2016). The study area covered approximately 25% of the total area of the NCHA, amounting to 47,310 km^2. Its geographical coordinates range between longitude 7°39'E – 9°52'E and latitude 4°36'*N* – 7°35'N, and its topography ranges between 19 and 931 m above sea level. Figure 1 shows the location of the study area in Nigeria.

2.2 Data collection

The data collected for this study included ground observations from five gauging stations, CHIRPS 2.0, CPC-CMORPH, GPM-IMERG07, and PERSIANN-CDR, downloaded in NetCDF file format, covering the entire globe. Table 1 shows the detailed information of the selected SPPs.

2.2.1 Rainfall data

The observed rainfall data used in this study were collected for five gauging stations from the Nigerian Meteorological Agency (NIMET) located in Oshodi, Lagos State, Nigeria. The 10 years daily data spanned from 1 January 2013 to 31 December 2022. The available gauging stations in the study area are limited and sparsely distributed. The temporal pattern of rainfall at all gauging stations showed that a significant amount of rainfall occurred between April and October, whereas little or no rainfall occurred between November and March. The completeness of the rainfall data records was checked, and it was observed that all gauging stations had few missing data, except for the Baro rain gauge station, which was collected from the Automated Weather Station (AWOS). Table 2 shows the geographical characteristics of the gauging stations, including the percentage of missing data and the mean annual rainfall. Figure 2 shows the temporal pattern of the rainfall at each gauging station for the considered duration.

2.2.2 Climate hazards group infrared precipitation with station data (CHIRPS)

CHIRPS, a quasi-global rainfall dataset, was developed by the U.S. Geological Survey Earth Resources Observation and Science (EROS) Centre in conjunction with the Santa Barbara Climate Hazards Group at the University of California. The development was to provide up-to-date, reliable data for early warning purposes, such as trend analysis and seasonal drought monitoring, by integrating in-situ datasets, reanalysis, and multiple satellite observations (Funk et al. 2015). The CHIRPS dataset includes precipitation information from 1981 to the present and offers various temporal series, including daily, pentad, and monthly precipitation at spatial resolutions of 0.05° and 0.25°. Daily data are considered real-time data with a 2-day latency period, whereas pentadal and monthly data are post-real-time data with a 21-day latency period. The CHIRPS algorithm uses the cold cloud duration (CCD) and ground gauge observations to approximate rainfall (Funk et al. 2015). Global daily CHIRPS version 2 at 0.25° spatial resolution was obtained for this study from https://data.chc.ucsb.edu/products/CHIRPS-2.0/global_daily/netcdf/ on 20 October 2023.

2.2.3 Climate prediction center (CPC) MORPHing technique (CMORPH)

CMORPH, developed by the Climate Prediction Centre, boasts a remarkable spatial resolution of 8 km at the equator and a temporal resolution of 30 min. The techniques used to develop these products involve utilizing low-orbiter satellite passive microwave (PMW) data to generate

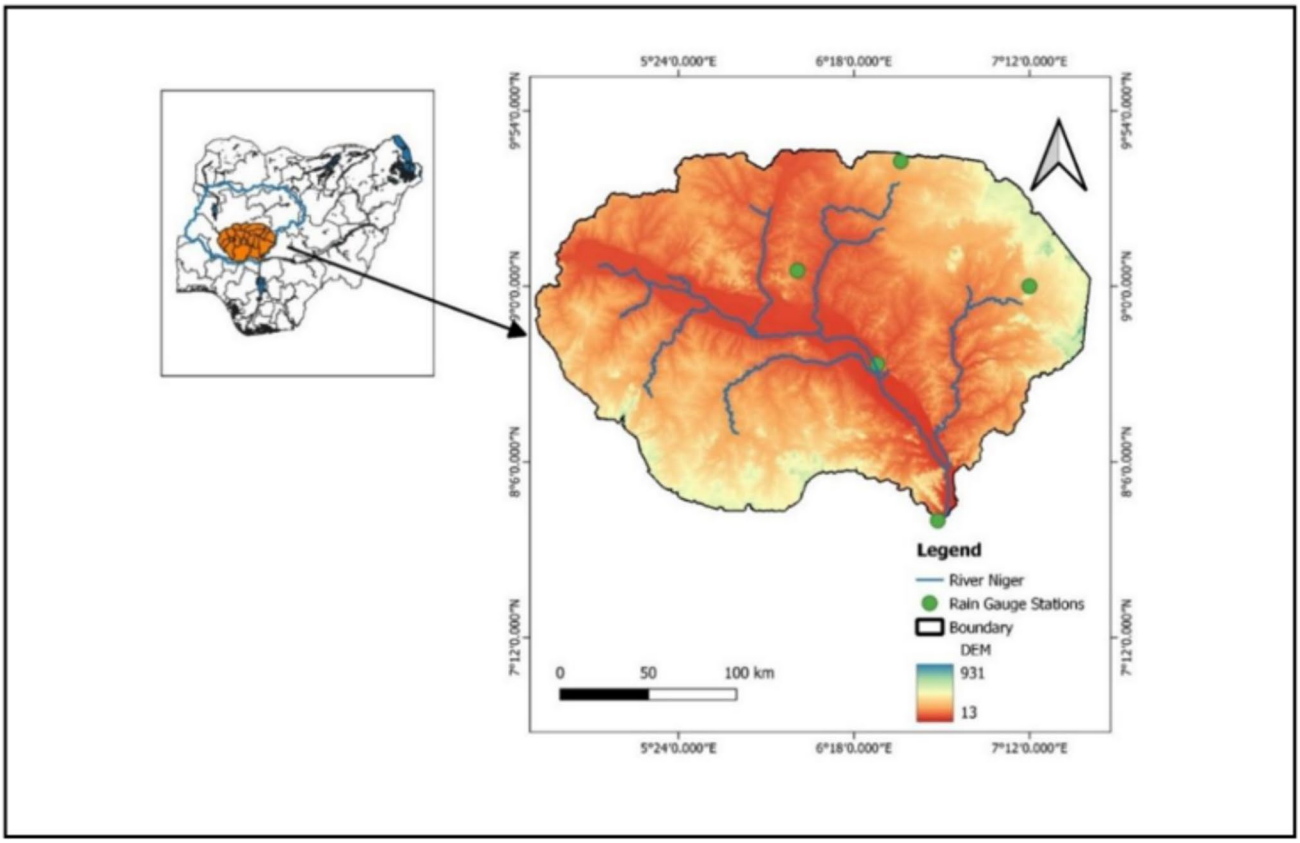


Fig. 1 Geographical location and elevation of the study rain gauge stations

precipitation estimates (Joyce et al. 2004). In addition, IR estimates are employed to transport the microwave-derived precipitation features during periods when microwave data is unavailable (Qin et al. 2014). For this study, the global daily CPC-CMORPH with a spatial resolution of 0.25° was obtained from https://www.ncei.noaa.gov/data/cmorph-high-resolution-global-precipitation-estimates/access/daily/ on 24 October 2023.

Table 1 Data information on the satellite precipitation products

S/*N*	Datasets	Period	Spatial Coverage	Spatial Resolution	Temporal Resolution
1	CHIRPS2.0	2013–2022	50°N – 50°S	0.05°	Daily
2	CPC-CMORPH	2013–2022	60°N – 60°S	0.25°	Daily
3	GPM-IMERG07	2013–2022	90°N – 90°S	0.1°	Daily
4	PERSIANN-CDR	2013–2022	60°N – 60°S	0.25°	Daily
5	Ground Observation	2013–2022	Niger Basin	Point	Daily

Table 2 Geographical characteristics of the gauge stations with percentage of missing data and mean annual rainfall

S/*N*	Station	Longitude (°E)	Latitude (°*N*)	Elevation (m)	% missing	Mean Annual Rainfall (mm)
1	Abuja	7.2	9	344	0.739	1216.29
2	Baro	6.42	8.6	60	0.000	658.02
3	Bida	6.01	9.08	143	0.329	1260.15
4	Lokoja	6.73	7.8	44	0.383	1288.88
5	Minna	6.54	9.64	260	0.329	1289.68

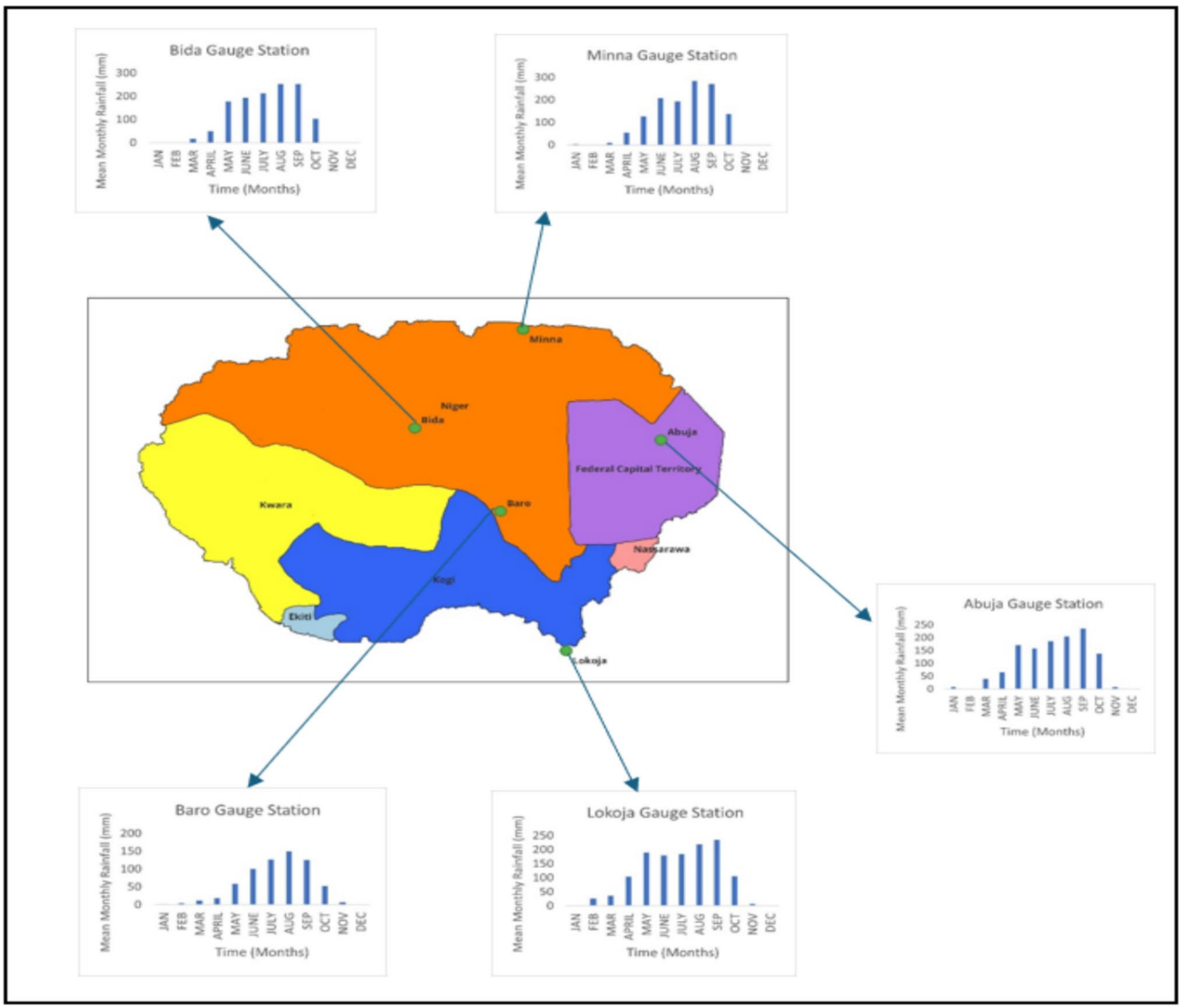


Fig. 2 Temporal pattern of rainfall at each gauge station

2.2.4 Integrated multi-satellite retrievals for global precipitation measurement (IMERG)

IMERG was produced by the National Aeronautics and Space Administration (NASA) and estimates global surface precipitation at a high resolution of 0.1° every half hour, starting in 2000. As part of the joint NASA and Japan Aerospace Exploration Agency (JAXA) Global Precipitation Measurement (GPM) mission, the GPM Core Observatory satellite was used as a standard to combine precipitation observations from international satellite constellations using advanced techniques. IMERG can be utilized for a variety of global-scale applications as well as for regions with sparse or no reliable ground observations. The high spatial and temporal resolution of IMERG data enables it to accumulate increased skills at the application scale. IMERG is categorized into three runs with varying latencies in response to a range of application requirements: rapid-response applications (Early Run, 4-h latency), same/next-day applications (Late Run, 14-h latency), and post-real-time research (Final Run, 3.5-month latency). The latest upgraded version of the IMERG product, GPM Level 3 IMERG Final Daily 10 × 10 km (GPM_3IMERGDF) was derived from the half-hourly GPM_3IMERGHH and supersedes all the previous versions of the IMERG products. The Retrospective Processing for the Final Run began on 1 July 2023 and was completed on 30 August 2023 (Huffman et al. 2023). This product was obtained from https://disc.gsfc.nasa.gov/datasets/GPM_3IMERGDF_07/summary?keywords=GPM_IMERG%20Final on 25 October 2023.

2.2.5 Precipitation estimation from remotely sensed information using artificial neural networks-climate data record (PERSIANN-CDR)

PERSIANN-CDR was developed by the Center for Hydrometeorology and Remote Sensing (CHRS) at the University of California to provide consistent, long-term, and high-resolution global precipitation data for climatic and hydrological studies, particularly extreme precipitation events. PERSIANN-CDR was developed from the PERSIANN algorithm employing GridSat-B1 infrared data, and the model outputs were corrected using the monthly Global Precipitation Climatology Project (GPCP) product to minimize biases in the estimated precipitation (Sun et al. 2018). The PERSIANN applies an artificial neural network (ANN) model to estimate precipitation using IR, enhancing the accuracy by adjusting the network parameters using TRMM Microwave Imager (TMI) rainfall estimates (Thiemig et al. 2012). Daily PERSIANN-CDR at 0.25° spatial resolution was downloaded from https://www.ncei.noaa.gov/data/precipitation-persiann/access/ on 27 October 2023.

2.3 Data processing

Data processing, analysis, and visualization were carried out using Microsoft Excel, R version 4.3.1 (Core Team 2019) in the Rstudio environment (RStudio Team 2019), an open-source Quantum Geographical Information System (QGIS version 3.14.1; QGIS Team 2019) to produce map layers, Climate Data Operators (CDO; Uwe 2018) to manipulate and analyze SPPs in NetCDF using a collection of command line operators, and RHtests_dlyPrcp obtained from http://etccdi.pacificclimate.org/software.shtml to confirm the consistency and homogeneity of ground observations. This software was specifically designed to homogenize daily precipitation data (Wang et al. 2010). SPPs with a spatial resolution of less than or greater than 0.1° were resampled to 0.1° using the bilinear interpolation method for fair comparison. There are two methods to compare SPPs with ground observations. These methods are grid-to-grid and point-to-grid (Ayehu et al. 2018). This study employed the latter option by extracting precipitation values from grids corresponding to five gauging stations and comparing them with daily ground observations. This approach was adapted by Ayehu et al. (2018), Dinku et al. (2014), Mianabadi (2023), and Pereira et al. (2024) due to the varying spatial resolutions of the applied SPPs.

2.4 Statistical evaluation of SPPs performance

The performance of the SPPs against ground observations was evaluated using scatter plot analysis, descriptive statistics, categorical statistics, and bias decomposition.

2.4.1 Scatterplots

Daily pixel-extracted SPPs (CHIRPS2.0, CPC-CMORPH, GPM-IMERG07, and PERSIANN-CDR) were evaluated against coinciding daily ground observations at each gauging station using scatterplots to measure the coefficient of determination (R^2). This process was repeated at monthly temporal resolution. Monthly data were obtained by aggregating the daily precipitation data.

2.4.2 Descriptive statistics

The descriptive statistics used for the comparison of SPPs against ground observations at daily and monthly temporal resolutions are Pearson's product-moment correlation coefficient (R) for measuring the linear relationship, mean absolute error (MAE) for measuring the mean magnitude of errors without considering the direction, root mean square error (RMSE) indicating the mean absolute error, and bias for measuring the mean difference between the SPPs and ground observations.

2.4.3 Categorical statistics

Categorical statistics were used to assess the efficiency of the SPPs by measuring their capacity to detect rainfall events. The categorical statistics applied in this study included Accuracy (ACC), Probability of Detection (POD), False Alarm Ratio (FAR), Critical Success Index (CSI), and Heidke Skill Score (HSS). These statistics were computed using combinations of hit (H), miss (M), false alarm (FA), and correct negative (CN) to verify the correct and incorrect rainfall detection frequencies at a daily temporal resolution. H measures the correct detection of rainfall by SPPs and ground observations, M measures the detection of rainfall by ground observations but fails by SPPs, FA measures the detection of rainfall by SPPs but fails by ground observations, and CN measures no detection of rainfall by SPPs and ground observations. The combinations were represented by a 2×2 contingency table (refer Table 3), applying a threshold of 1 mm per day to define rainy days. The threshold used in this study was adopted from the studies by Dinku et al. (2018) and Zhang et al. (2021).

Table 3 Contingency table of rainfall events by SPPs and ground observations (Dinku et al. 2018 and Zhang et al. 2021)

		Satellite Precipitation	
		0	1
Ground Observed Rainfall	0	Corrective Negative (CN)	False Alarm (FA)
	1	Misses (M)	Hits (H)

2.4.4 Bias decomposition

The total bias in SPPs was quantified using the 4CED developed by Zhang et al. (2021) to measure HPB, HNB, FB, and MB. HPB and HNB represent the overestimation and underestimation of precipitation correctly detected by SPPs and ground observations, respectively. Conversely, FB represents precipitation detection by SPPs, but no record of precipitation by ground observation, whereas MB represents the opposite scenario of FB. Among the four independent error components, HPB and FB are always positive, whereas HNB and MB are always negative (Li et al. 2023). This may result in a smaller magnitude of total bias (TB) where positive and negative individual components cancel each other (Zhang et al. 2021).

Table 4 lists the statistical evaluation indices applied in this study to evaluate the suitability of SPPs.

3 Results and discussion

3.1 Spatial-temporal variation of ground observations and SPPs

The mean annual rainfall of ground observations, CHIRPS2.0, CPC-CMORPH, GPM-IMERG07, and PERSIANN-CDR were represented with spatial maps to show the pattern of rainfall for 10 years (2013–2022) in the study area as presented in Fig. 3. Ground observations showed a decreasing pattern of rainfall from the North and South to the central part of the basin, whereas CHIRPS2.0, CPC-CMORPH, and PERSIANN-CDR followed the same pattern from the West and East to the central part of the basin. In the case of GPM-IMERG07, a decreasing rainfall pattern was observed from the East to the West of the basin. The mean annual rainfall of ground observations, CHIRPS2.0, CPC-CMORPH, GPM-IMERG07, and PERSIANN-CDR were 1104.70, 1189.39, 852.08, 1202.26, and 1240.97 mm, respectively, with PERSIANN-CDR and CPC-CMORPH having the highest and lowest

Table 4 Statistical evaluation indices for determining the suitability of SPPs (Dinku et al. 2018; Helmi and Abdelhamed 2023; Li et al. 2023)

S/*N*	Statistical Indices	Formulas	Unit	Range	Perfect Value
1.	Pearson Correlation Coefficient (R)	$\frac{\sum_{i=1}^{n}\left(P_{gi}-\overline{P}_{g}\right)\left(P_{si}-\overline{P}_{s}\right)}{\sqrt{\left(P_{gi}-\overline{P}_{g}\right)^{2}}\sqrt{\left(P_{si}-\overline{P}_{s}\right)^{2}}}$		−1–1	1
2.	Mean Absolute Error (MAE)	$\frac{1}{n}\sum_{i=1}^{n}\left\|P_{si}-P_{gi}\right\|$	mm	0 - ∞	0
3.	Root Mean Square Error (RMSE)	$\sqrt{\frac{1}{n}\sum_{i=1}^{n}\left(P_{si}-P_{gi}\right)^{2}}$	mm	0 - ∞	0
4.	BIAS	$\sum_{i=1}^{n}\left(P_{si}-P_{gi}\right)$		-∞ - +∞	0
5.	Accuracy (ACC)	$\frac{H+CN}{H+CN+FA+M}$		0–1	1
6.	Probability of Detection (POD)	$\frac{H}{H+M}$		0–1	1
7.	False Alarm Ration (FAR)	$\frac{FA}{H+FA}$		0–1	0
8.	Critical Success Index (CSI)	$\frac{H}{H+M+FA}$		0–1	1
9.	Heidke Skill Score (HSS)	$\frac{2(H\times CN-FA\times M)}{((H+M)(M+CN)+(H+FA)(FA+CN))}$		-∞ − 1	1
10.	Hit Positive Bias (HPB)	$\frac{\sum_{i=1}^{hp}\left(P_{si}-P_{gi}\right)}{\sum_{i=1}^{n}G}$		0 - ∞	0
11.	Hit Negative Bias (HNB)	$\frac{\sum_{i=1}^{hn}\left(P_{si}-P_{gi}\right)}{\sum_{i=1}^{n}G}$		0 - ∞	0
12.	False Bias (FB)	$\frac{\sum_{i=1}^{f}\left(P_{si}-P_{gi}\right)}{\sum_{i=1}^{n}G}$		0 - ∞	0
13.	Miss Bias (MB)	$\frac{\sum_{i=1}^{m}\left(P_{si}-P_{gi}\right)}{\sum_{i=1}^{n}G}$		0 - ∞	0
14.	Total Bias	$HPB+HNB+MB+FB$		0 - ∞	0

*P represents precipitation,$\overline{P}$represents average precipitation, s and g represent SPPs and gauges, respectively. n is the number of precipitation events. f, m, hp, and hn represent the number of false, miss, hit positive, and hit negative precipitation events, respectively.

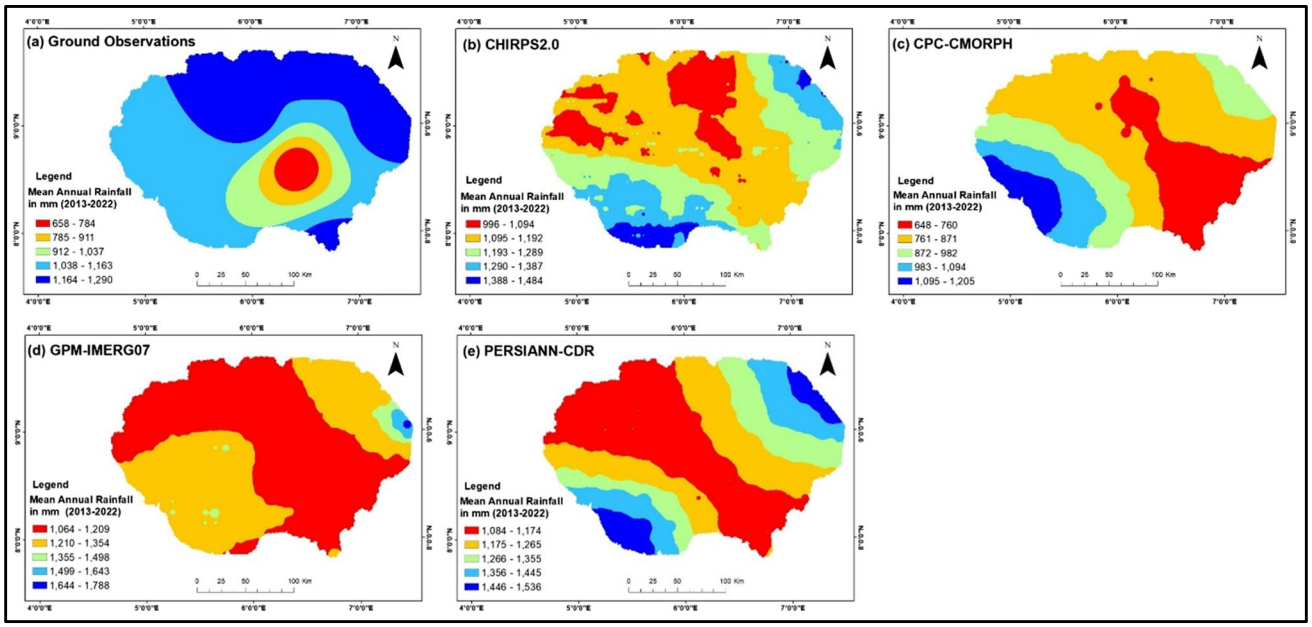


Fig. 3 Spatial maps of the mean annual rainfall of (**a**) ground observations, (**b**) CHIRPS2.0, (**c**) CPC-CMORPH, (**d**) GPM-IMERG, and (**e**) PERSIANN-CDR for 10 years (2013–2022)

mean annual rainfall, respectively. The temporal patterns of ground observations and SPPs were assessed by plotting a graphical representation of the mean monthly precipitation at each rain gauge station for 2013–2022 to show precipitation variability. The graphical plots (Fig. 4) revealed that the SPPs and ground observations followed the same pattern of low precipitation distribution during January, February, March, November, and December. This temporal variation is consistent with a similar study conducted in Nigeria by Akinyemi et al. (2020), using different datasets (TRMM, CHIRPS, and RFE against gauge rainfall data), gauging stations, and time durations. All SPPs, except for CPC-CMORPH, had a rainfall pattern similar to that of ground observations at the five gauging stations. However, CPC-CMORPH had a higher level of agreement with ground observations at the Baro gauge station, whereas the other SPPs overestimated the ground observations. Peak rainfall was observed in August and September, except for CPC-CMORPH at the Abuja and Lokoja rain gauge stations and CHIRPS2.0 at the Abuja, Baro, and Bida rain gauge stations, which showed a significant decline in precipitation in September. Climate variability can significantly influence precipitation patterns, altering weather systems and causing some regions to experience changes in rainfall. September often represents a transitional period between climatic seasons in many areas, leading to seasonal trends and irregularities. These changes in precipitation are more observable in high-resolution datasets like CHIRPS2.0 (Funk et al. 2015), which combines satellite imagery with ground station data. Nevertheless, inaccuracies in either data source can affect the merged product, especially during months with significant variability (Touma et al.,2023).

3.2 Evaluation of SPPs against ground observed rainfall using scatter plots

3.2.1 Daily scatter plot evaluation

The daily comparison between the four SPPs (CHIRPS2.0, CPC-CMORPH, GPM-IMERG07, and PERSIANN-CDR) against ground observations at each gauging station was visualized through graphs using scatterplots, as shown in Fig. 5. The coefficient of determination, R^2, varied from station to station, with weak positive R^2 values ranging between 0.04 and 0.19. GPM-IMERG07 exhibited the highest R^2 value at the Bida rain gauge station. This was followed by CPC-CMORPH at the Bida rain gauge station with an R^2 value of 0.15, whereas CPC-CMORPH and GPM-IMERG07 had the lowest R^2 value of 0.04 at the Baro rain gauge station. Generally, GPM-IMERG07 and PERSIANN-CDR performed better than the other SPPs, with weak coefficients of determination ($R^2 < 0.5$). A weak positive R^2 in the daily comparison agreed with similar findings in Nigeria (Salami and Fenta 2022), the Black Volta Basin in West Africa (Adjei et al. 2015), and Burkina Faso (Dembélé and Zwart 2016).

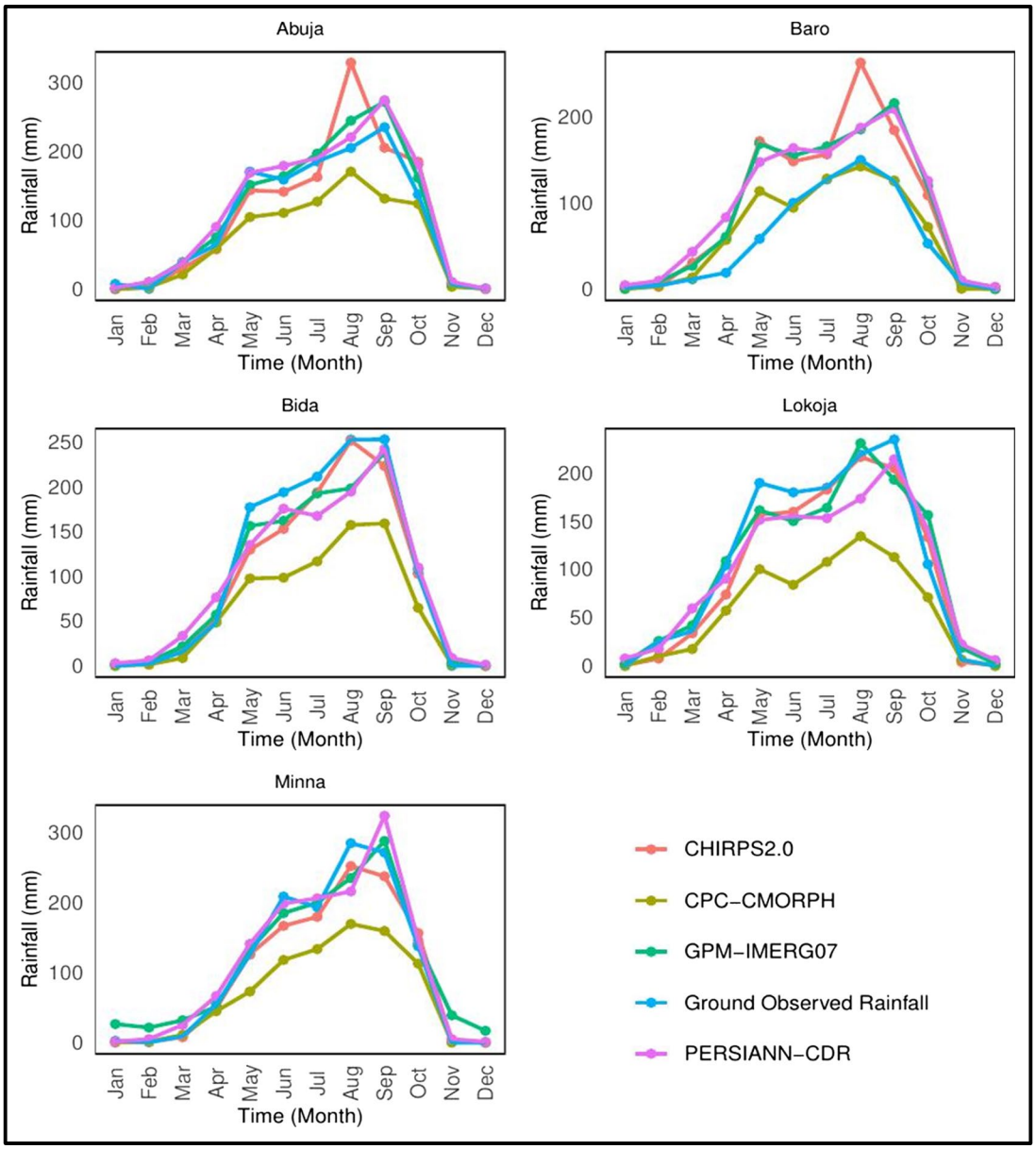


Fig. 4 Mean monthly variability of the SPPs and ground observations at each gauge station

3.2.2 Monthly scatter plot evaluation

Relative to the daily evaluation, the coefficient of determination (R^2) between the monthly SPPs and ground observations from the aggregated daily precipitation data showed significant improvement across the five gauging stations, with R^2 values ranging between 0.54 and 0.86. CHIRPS2.0 and GPM-IMERG07 recorded the lowest and highest values of R^2 at the Abuja and Bida rain gauge stations, respectively. This result agreed with the findings of Gunathilake et al. (2020), with GPM-IMERG07 showing superiority over the others at daily and monthly temporal resolutions. However, in general terms, it was observed that PERSIANN-CDR reproduced ground observations better than the other SPPs. In addition, its high performance was also observed across all gauging stations ($R^2 > 0.7$). Figure 6 presents scatter plots of SPPs against ground observations at each gauging station. This improvement in R^2 monthly over daily was mainly due to temporal data aggregation such that positive errors cancelled negative errors (Adjei et al. 2015).

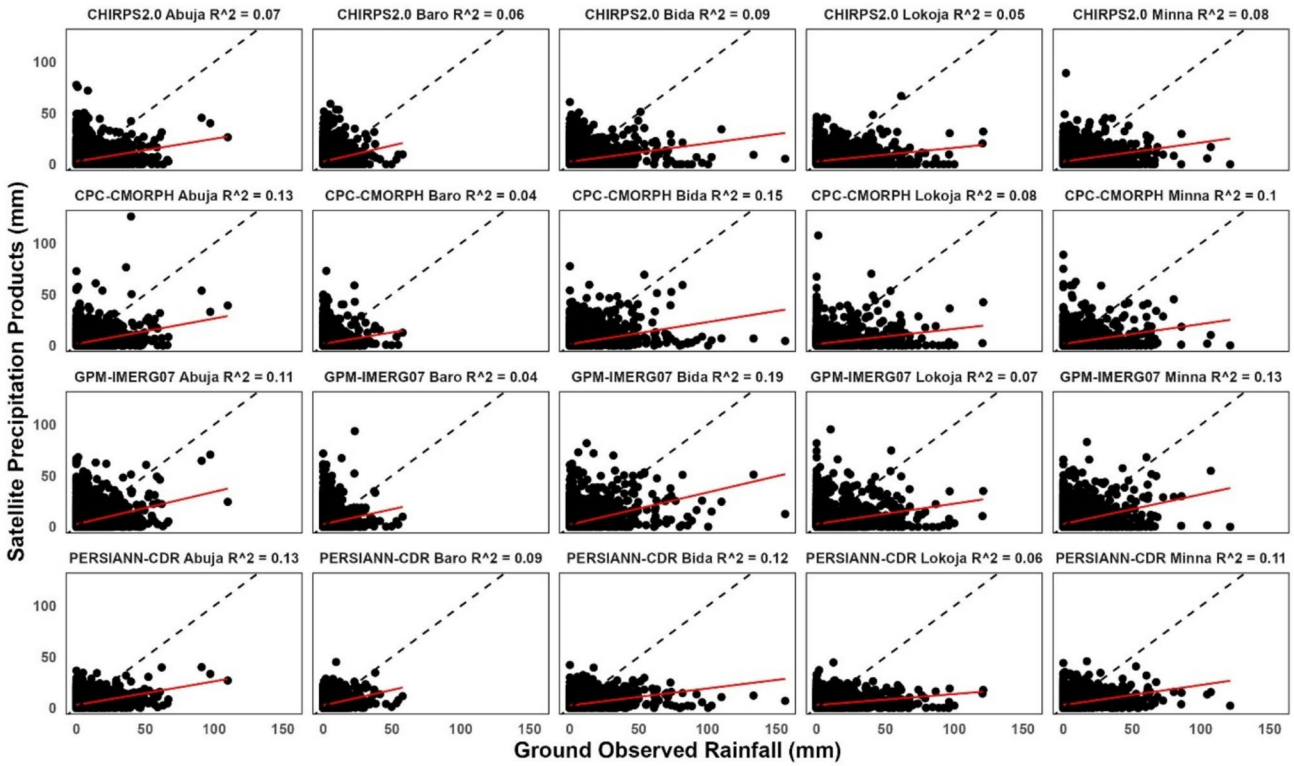


Fig. 5 Scatter plots of daily SPPs against ground observations at each gauge station

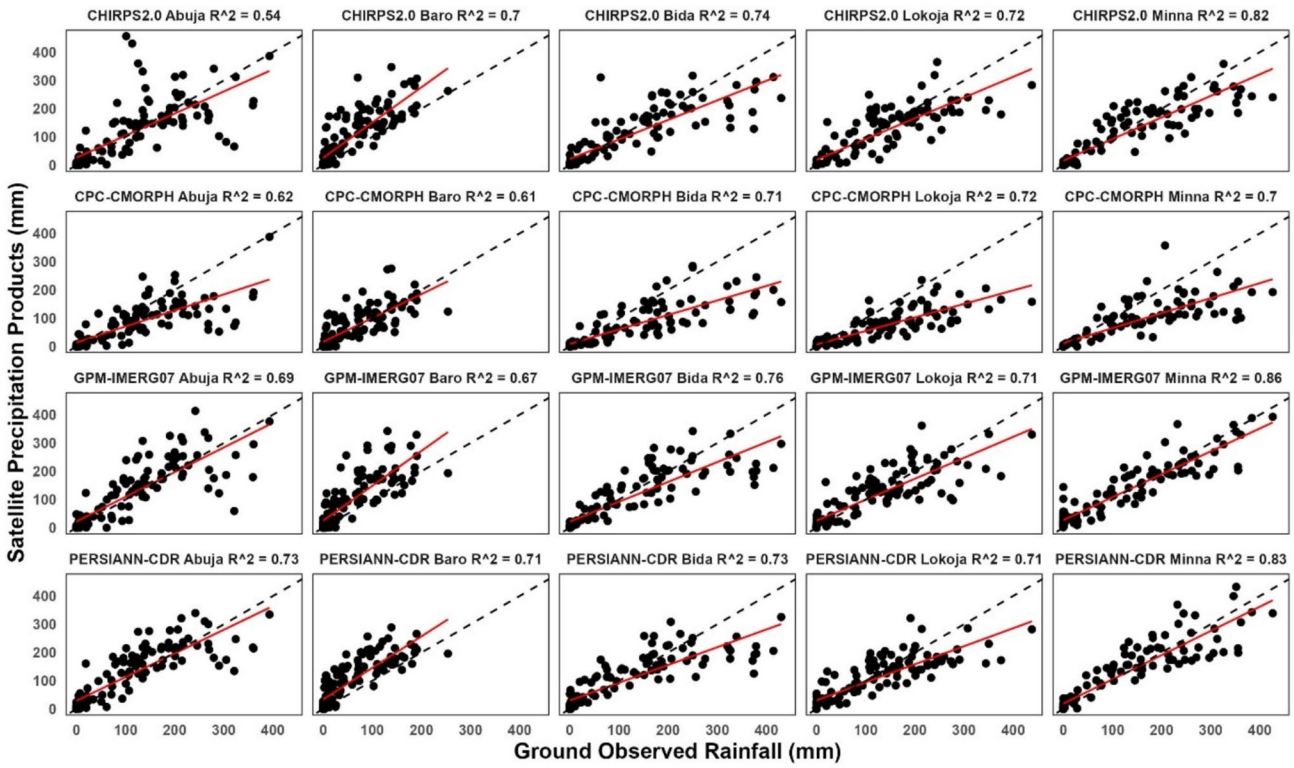


Fig. 6 Scatter plots of monthly SPPs against ground observations at each gauge station

Table 5 Descriptive statistics of daily SPPs at each gauging station

Station	SPPs	*R*	MAE	RMSE	Bias
Abuja	CHIRPS2.0	0.27	4.44	9.71	−0.15
	CPC-CMORPH	0.36	3.59	8.79	0.97
	GPM-IMERG07	0.34	4.29	9.81	−0.31
	PERSIANN-CDR	0.36	4.26	8.53	−0.42
Baro	CHIRPS2.0	0.24	3.43	7.22	−1.30
	CPC-CMORPH	0.20	2.67	6.59	−0.26
	GPM-IMERG07	0.19	3.46	8.20	−1.25
	PERSIANN-CDR	0.30	3.14	6.05	−1.33
Bida	CHIRPS2.0	0.30	4.28	10.90	0.34
	CPC-CMORPH	0.39	3.36	10.23	1.38
	GPM-IMERG07	0.43	3.67	10.30	0.31
	PERSIANN-CDR	0.35	4.18	10.27	0.29
Lokoja	CHIRPS2.0	0.23	4.91	11.50	0.31
	CPC-CMORPH	0.29	3.90	10.97	1.60
	GPM-IMERG07	0.27	4.79	11.79	0.08
	PERSIANN-CDR	0.24	4.90	11.03	0.26
Minna	CHIRPS2.0	0.29	4.29	10.08	0.30
	CPC-CMORPH	0.32	3.69	9.86	1.27
	GPM-IMERG07	0.36	4.41	10.29	−0.22
	PERSIANN-CDR	0.33	4.38	9.66	−0.13

3.3 SPPs evaluation using descriptive statistics

3.3.1 Daily descriptive statistics

The results of the point-wise comparison between the four SPPs (CHIRPS2.0, CPC-CMORPH, GPM-IMERG07, and PERSIANN-CDR) and the daily ground observed rainfall from the five gauging stations using descriptive statistics are presented in Table 5. It was observed that the coefficient of correlation, R varied between 0.19 and 0.43, with GPM-IMERG07 having the lowest value of R, at Baro rain gauge station but the highest at Bida rain gauge station. In a study by de Carvalho et al. (2017), Pearson's correlation is classified as weak when its value is less than 0.2, moderate when it falls between 0.2 and 0.5, and strong when it exceeds 0.5. Based on this classification, all the SPPs across the gauging stations were moderately correlated with the ground observations, except for GPM-IMERG07 at the Baro rain gauge station which was classified as weak. MAE varied between 2.67 and 4.91 mm, with CPC-CMORPH having the lowest MAE value at the Baro rain gauge station while CHIRPS2.0 had the highest MAE value at the Lokoja rain gauge station. In the case of RMSE, PERSIANN-CDR had the lowest value of 6.05 mm, while GPM-IMERG07 had the highest value of 11.79 mm at the Baro and Lokoja rain gauge stations, respectively. For Bias, GPM-IMERG07 and CPC-CMORPH had the lowest and highest values of 0.08 and 1.6, respectively, at the Lokoja rain gauge station. The results revealed that all SPPs underestimated precipitation at the Abuja rain gauge station, except for CPC-CMORPH, Baro rain gauge station, and Minna rain gauge station, except for CHIRPS2.0 and CPC-CMORPH.

A summary of the performance of the four daily SPPs against ground observations across the gauging stations is represented by box-and-whisker plots as shown in Fig. 7. The upper and lower edges of the box denote the upper and lower quartiles of 75% and 25%, respectively; the solid line within the box indicates the median value; the upper and lower horizontal lines extending beyond the box represent

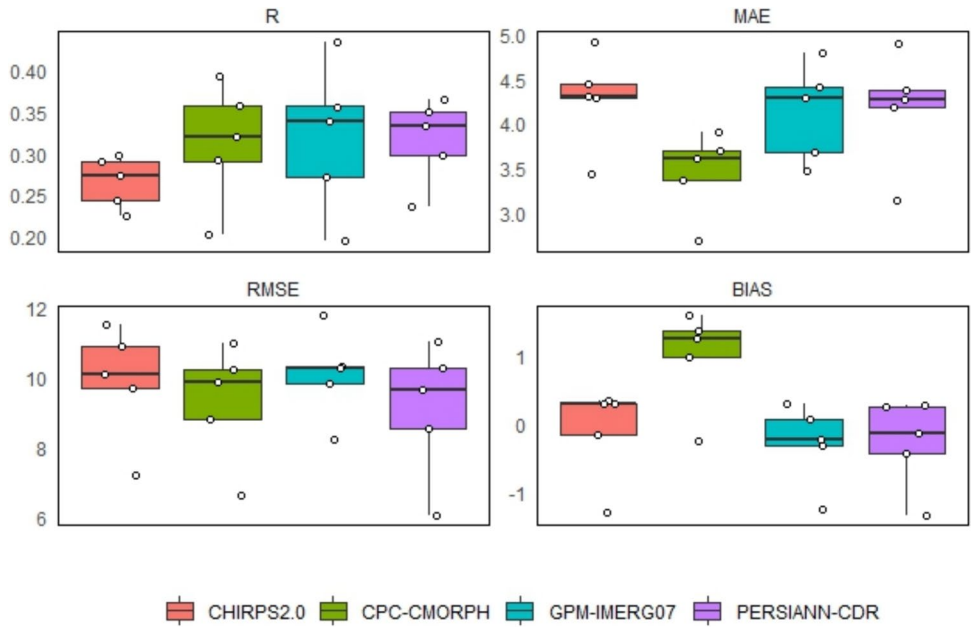


Fig. 7 Box and whiskers plot of the R, MAE, RMSE, and BIAS for the four daily SPPs against ground observations

the range of 1.5 IQR; and the individual data points are depicted with circles.

From the box and whisker plots, GPM-IMERG07 outperformed the other SPPs, with a median R-value of 0.34, followed by PERSIANN-CDR (0.33), CPC-CMORPH (0.32), and CHIRPS (0.27). For MAE, CPC-CMORPH performed better, with the lowest median MAE of 3.59 mm. This was followed by PERSIANN-CDR (MAE = 4.26 mm), CHIRPS2.0, and GPM-IMERG07, which had the same MAE value of 4.29 mm. However, PERSIANN-CDR performed best in the case of RMSE and BIAS, with the lowest median values of 9.66 mm and 0.13 (underestimation), respectively. CPC-CMORPH outperformed other SPPs next to PERSIANN-CDR for RMSE but performed poorly for BIAS, whereas the vice versa was for GPM-IMERG07. According to Helmi and Abdelhamed (2023), RMSE is the most used statistical parameter to quantify the errors in SPPs, where the smallest value of RMSE is selected as the best-performing satellite precipitation product. This was also demonstrated by Ji et al. (2022). Therefore, for evaluating daily SPPs, PERSIANN-CDR conformed to this submission with the lowest RMSE value. In addition, the high performance of PERSIANN-CDR was also observed in the other statistical metrics used in this study.

Table 6 Descriptive statistics of monthly SPPs at each gauging station

Station	SSP	R	MAE	RMSE	Bias
Abuja	CHIRPS2.0	0.73	42.80	77.19	4.46
	CPC-CMORPH	0.79	41.52	69.87	-29.63
	GPM-IMERG07	0.83	38.11	61.21	9.36
	PERSIANN-CDR	0.86	38.07	55.92	12.89
Baro	CHIRPS2.0	0.84	41.96	65.68	39.69
	CPC-CMORPH	0.78	27.05	42.84	7.82
	GPM-IMERG07	0.82	42.94	66.69	37.98
	PERSIANN-CDR	0.84	43.25	60.19	40.56
Bida	CHIRPS2.0	0.86	36.17	62.30	-10.39
	CPC-CMORPH	0.84	49.01	81.89	-41.98
	GPM-IMERG07	0.87	35.73	60.18	-9.40
	PERSIANN-CDR	0.86	39.73	64.35	-8.72
Lokoja	CHIRPS2.0	0.85	36.93	55.78	-9.32
	CPC-CMORPH	0.85	52.53	79.27	-48.74
	GPM-IMERG07	0.85	37.54	55.86	-2.50
	PERSIANN-CDR	0.84	40.52	57.59	-7.84
Minna	CHIRPS2.0	0.90	31.88	51.75	-9.01
	CPC-CMORPH	0.83	47.22	79.13	-38.53
	GPM-IMERG07	0.93	32.62	45.02	6.78
	PERSIANN-CDR	0.91	32.69	48.16	4.02

3.3.2 Monthly descriptive statistics

The results showed that the monthly SPPs were highly correlated with ground observations across the gauging stations, with R ranging between 0.73 and 0.93. GPM-IMERG07, PERSIANN-CDR, and CHIRPS2.0 at the Minna rain gauge station were highly correlated with ground observations ($R \geq 0.90$), while CHIRPS2.0 had the lowest correlation (R) of 0.73 at the Abuja rain gauge station. MAE ranged from 27.05 to 52.53 mm, with CPC-CMORPH having the lowest and highest values at Baro and Lokoja rain gauge stations, respectively. The RMSE values ranged from 42.84 to 79.27 mm, with CPC-CMORPH having the lowest and highest values at the Baro and Lokoja rain gauge stations, respectively. Regarding bias, the values ranged from 2.5 to 48.74, with GPM-IMERG07 and CPC-CMORPH having the lowest and highest underestimated values at the Lokoja gauge station.

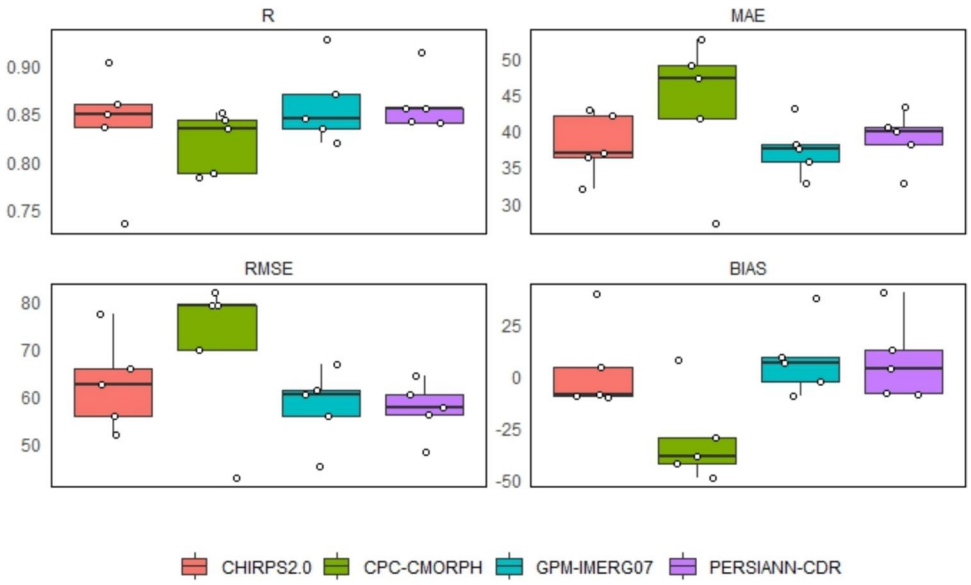


Fig. 8 Box and whiskers plot of the R, MAE, RMSE, and BIAS for the four monthly SPPs against ground observations

In contrast to the daily comparison, all SPPs overestimated precipitation at the Abuja rain gauge station, except for CPC-CMORPH, Baro rain gauge station, and Minna rain gauge station, except for CHIRPS2.0 and CPC-CMORPH. The detailed descriptive performance of the SPPs at each gauging station is presented in Table 6.

A summary of the monthly descriptive statistics is presented in Fig. 8, using box-and-whisker plots. PERSIANN-CDR outperformed the other SPPs, with a median R value of approximately 0.86, whereas CPC-CMORPH had the lowest median R value of approximately 0.83. In the case of MAE, CHIRPS2.0 performed better than the other SPPs, followed by GPM-IMERG07 and PERSIANN-CDR. In contrast, in the case of RMSE and Bias, the SPPs followed the same pattern of performance, with PERSIANN-CDR outperforming other SPPs, while CPC-CMORPH recorded the lowest performance. Moreover, it was observed that CHIRPS2.0 and CPC-CMORPH underestimated precipitation. Based on the justification provided for the daily descriptive statistics, PERSIANN-CDR was the SPP most correlated with ground observations and performed better than other SPPs, having the lowest median RMSE value of approximately 57.59 mm and recording a relatively high performance in other metrics.

3.4 Categorical statistics

A high accuracy (ACC) of the SPPs was recorded at all gauge stations, ranging from approximately 0.65 to 0.85. CPC-CMORPH outperformed the other SPPs at the Bida rain gauge station, whereas PERSIANN-CDR recorded the lowest performance at the Lokoja rain gauge station. The probability of detection (POD) varied between 0.56 and 0.89. PERSIANN-CDR and CHIRPS2.0 had the strongest (above 0.75) and least detection probabilities at all gauging stations. CPC-CMORPH had the lowest (best) value of the false alarm ratio (FAR), whereas PERSIANN-CDR had the worst false rainfall detection at all gauging stations. A low critical success index (CSI) was observed at all stations ranging from 0.3 to 0.49, with CPC-CMORPH having the highest CSI at Bida, Lokoja, and Minna rain gauge stations, GPM-IMERG07 at Abuja rain gauge station, and PERSIANN-CDR at Baro rain gauge station, while CHIRPS2.0 was the lowest at all the gauging stations. CPC-CMORPH had better HSS performance across the gauging stations, whereas CHIRPS and PERSIANN-CDR performed poorly at the Lokoja rain gauge station. Generally, it was observed that CPC-CMORPH performed consistently at all the gauging stations in terms of ACC, FAR, HSS, and PERSIANN-CDR in terms of POD, whereas other SPPs performed differently. The details of the categorical statistics for daily SPPs at each gauging station are presented in Table 7.

The mean categorical statistics (ACC, POD, FAR, CSI, and HSS) for all the SPPs are shown in Fig. 9. The SPPs; CHIRPS2.0, CPC-CMORPH, GPM-IMERG07, and PERSIANN-CDR showed an overall good performance (ACC = 0.75, 0.81, 0.78, and 0.70; POD = 0.64, 0.66, 0.72, and 0.85; FAR = 0.54, 0.45, 0.51, and 0.58; CSI = 0.37,

Table 7 Categorical statistics of daily SPPs at each gauging station

Stations	SPPs	ACC	POD	FAR	CSI	HSS
Abuja	CHIRPS2.0	0.74	0.65	0.50	0.39	0.39
	CPC-CMORPH	0.79	0.67	0.42	0.45	0.48
	GPM-IMERG07	0.78	0.73	0.45	0.46	0.47
	PERSIANN-CDR	0.70	0.88	0.54	0.43	0.40
Baro	CHIRPS2.0	0.73	0.57	0.57	0.33	0.31
	CPC-CMORPH	0.77	0.56	0.48	0.37	0.39
	GPM-IMERG07	0.76	0.61	0.50	0.37	0.39
	PERSIANN-CDR	0.70	0.80	0.58	0.38	0.35
Bida	CHIRPS2.0	0.78	0.70	0.53	0.39	0.42
	CPC-CMORPH	0.85	0.74	0.40	0.49	0.56
	GPM-IMERG07	0.83	0.80	0.45	0.49	0.54
	PERSIANN-CDR	0.73	0.89	0.58	0.40	0.40
Lokoja	CHIRPS2.0	0.73	0.60	0.63	0.30	0.29
	CPC-CMORPH	0.79	0.62	0.53	0.36	0.40
	GPM-IMERG07	0.79	0.74	0.59	0.36	0.37
	PERSIANN-CDR	0.65	0.82	0.67	0.31	0.27
Minna	CHIRPS2.0	0.77	0.70	0.49	0.42	0.44
	CPC-CMORPH	0.82	0.70	0.40	0.48	0.53
	GPM-IMERG07	0.73	0.74	0.54	0.39	0.38
	PERSIANN-CDR	0.73	0.88	0.54	0.43	0.42

0.43, 0.41, and 0.39; HSS = 0.37, 0.47, 0.43, and 0.37, respectively). However, all SPPs performed below the average perfect score of one (1) for CSI and HSS. The findings revealed that CPC-CMORPH had the highest ACC, CSI, and HSS, whereas PERSIANN-CDR demonstrated the lowest performance of ACC and CHIRPS2.0 had the lowest CSI and HSS compared to other SPPs. The CSI and HSS are typically intended to enhance analysis. However, these indices are heavily dependent on the FA and CN values, which are inadequately captured by the gauge network (Hussain et al. 2017a, b). PERSIANN-CDR had the highest mean POD and FAR, while CHIRPS2.0 and CPC-CMORPH had the lowest POD and FAR, respectively. A similar result of PERSIANN-CDR, with the highest values of POD and FAR at the daily temporal resolution, was observed by Helmi and Abdelhamed (2023) and Ji et al. (2022) in a study conducted in the Kingdom of Saudi Arabia and China, respectively. This is consistent with previous studies (Dinku et al. 2018; Qiu et al. 2014), which revealed that the SPP with the highest POD value had the highest FAR (i.e. best and poor performance, respectively).

Gebremedhin et al. (2021) and Rahmawati and Lubczynski (2018) indicated that FAR (having FA in both the numerator and denominator) is inadequate for evaluating SPP performance. This is because rainfall clouds may pass through an analyzed pixel without covering the ground observation, resulting in the gauge not recording any rainfall, even when rainfall is available in the pixel for satellite detection. It was observed that among the categorical statistics, only POD is reliable because it is independent of FA. This assertion was supported by Lekula et al. (2018), who highlighted the influencing factors of POD which are miss (M) and hit (H), ranking M as the most important factor in determining the best SPPs because it directly indicates satellite algorithm sensitivity to rainfall detection.

Therefore, based on references, PERSIANN-CDR emerged as the most suitable SPP because it significantly detected daily precipitation better in the study area than other SPPs.

3.5 SPPs evaluation of bias error decomposition using 4CED

The total bias (TB) and 4CED categorized as HPB, HNB, MB, and FB are presented in Table 8. PERSIANN-CDR showed the lowest HNB and MB values ranged from 456 to 557 mm and 82 to 173 mm, respectively, and the highest HPB and FB values ranged from 199 to 401 mm and 898 to1163 mm, respectively, at all gauging stations. Conversely, CPC-CMORPH exhibited the lowest values of HPB and FB ranging from 122 to 260 mm and 367 to 490 mm, respectively, and the highest HNB values ranged from 570 to 696 mm at all gauging stations and MB value of 374 mm at Bida station while CHIRPS2.0 had the highest MB values at the other four gauging stations, ranged from 222 to 330 mm. In the case of TB, GPM-IMERG07 had the lowest TB values of 23 mm, 0 mm, and 123 mm at Abuja, Baro, and Bida rain gauge stations, respectively, and CHIRPS2.0 had 109 mm and 31 mm at Lokoja and Minna rain gauge stations, respectively, while PERSIANN-CDR exhibited the highest TB values ranged from 598 to 736 mm at all the gauging stations. The results revealed that Hit and False errors constituted the major components of the total bias for the four SPPs at all the gauging stations. This result was consistent with the findings of Chen et al. (2021).

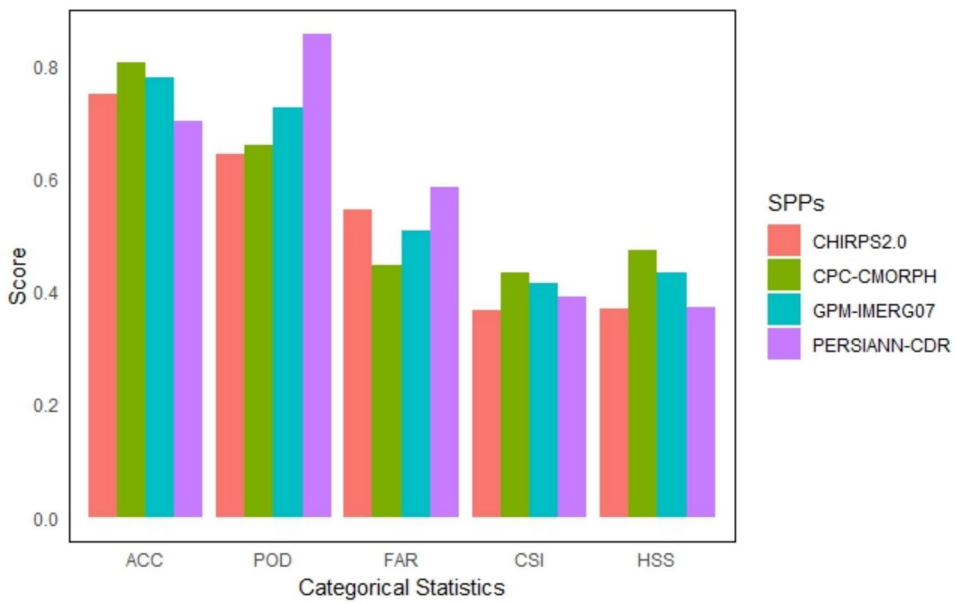


Fig. 9 Bar chart showing the mean ACC, POD, FAR, CSI, and HSS for CHIRPS2.0, CPC-CMORPH, GPM-IMERG07, and PERSIANN-CDR

Table 8 Bias error decomposition of daily SPPs at each gauging station

Station	SPPs	HPB	HNB	MB	FB	TB
Abuja	CHIRPS2.0	317	618	330	603	−28
	CPC-CMORPH	238	696	306	451	−313
	GPM-IMERG07	323	612	251	563	23
	PERSIANN-CDR	379	557	112	972	682
Baro	CHIRPS2.0	354	503	371	633	113
	CPC-CMORPH	260	595	374	450	−259
	GPM-IMERG07	332	525	337	530	0
	PERSIANN-CDR	401	456	173	934	706
Bida	CHIRPS2.0	251	492	222	593	130
	CPC-CMORPH	170	570	194	367	−227
	GPM-IMERG07	264	479	147	484	122
	PERSIANN-CDR	264	479	82	921	624
Lokoja	CHIRPS2.0	187	510	277	709	109
	CPC-CMORPH	122	574	266	490	−228
	GPM-IMERG07	186	512	184	740	230
	PERSIANN-CDR	199	499	127	1163	736
Minna	CHIRPS2.0	288	575	260	578	31
	CPC-CMORPH	196	665	257	406	−320
	GPM-IMERG07	275	587	222	765	231
	PERSIANN-CDR	332	530	102	898	598

*HPB and FB are positive, whereas HNB and MB are negative.

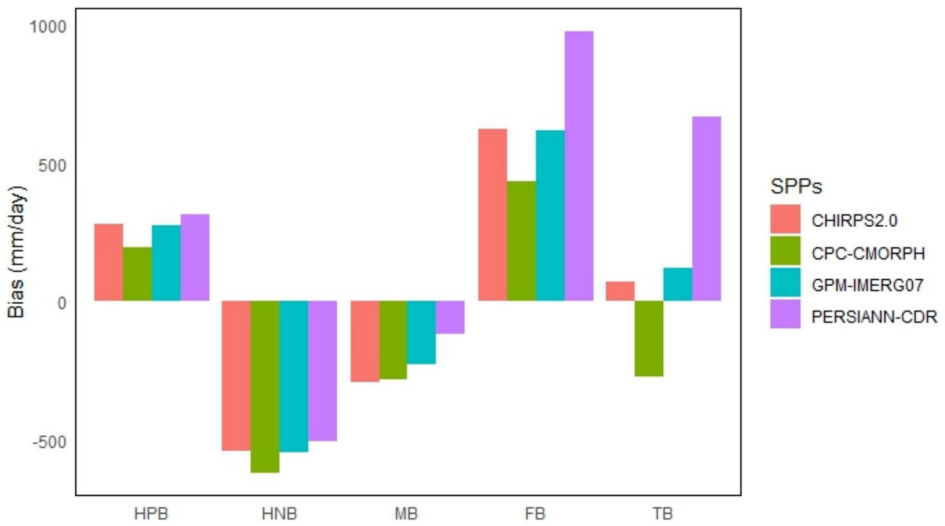


Fig. 10 The hit positive bias (HPB), hit negative bias (HNB), miss bias (MB), false bias, and total bias (TB) components for each satellite precipitation product (SPP) over the NCHA basin

The mean values of the total bias and the four error components of the bias decomposition for the four SPPs are shown in Fig. 10. Several studies have established that the lower the bias volume, the better the SPP. Generally, the HPB and FB followed the same performance pattern for all SPPs. CPC-CMORPH had the highest mean HNB value of 620 mm and the lowest mean HPB and FB values of 197 mm and 433 mm, respectively compared to the other SPPs. However, PERSIANN-CDR had the highest mean HPB, FB, and TB values of 315 mm, 578 mm, and TB 669 mm, respectively, and the lowest mean HNB and MB values of 504 mm and 119 mm, respectively. Whereas, CHIRPS2.0 had the lowest TB value of 71 mm.

The findings showed that the best performance of HNB and MB was observed in PERSIANN-CDR, HPB and FB in CPC-CMORPH, and TB in CHIRPS2.0. The TB for CHIRPS2.0 is negative, showing that it underestimates precipitation. According to Gebremedhin et al. (2021), FB,

which includes FA cannot be considered a reliable indicator, as explained in the categorical statistics section. In addition, FB is inconclusive regarding the validation of SPPs, although it influences total accumulated rainfall (Lekula et al. 2018). The influence of FB on TB was observed in PERSIANN-CDR, which resulted in the highest magnitude of TB. However, PERSIANN-CDR, which has the lowest amount of MB compared to the other SPPs, missed much less rainfall detected by ground observations.

4 Conclusion

This study evaluated the suitability of CHIRPS2.0, CPC-CMORPH, GPM-IMERG07, and PERSIANN-CDR against ground observations in a sparsely distributed data area covering five gauging stations for a period of 10 years (2013–2022). The study employed scatter plots and descriptive statistics to evaluate SPPs at daily and monthly temporal resolutions. In addition, the daily SPPs were further assessed using categorical statistics and 4CED. The study concluded that all the SPPs agreed better with the ground observations but possessed greater errors (MAE, RMSE, and Bias) at monthly compared to the daily temporal resolution at all gauging stations based on the median descriptive statistics. This may be due to the small sample size in the monthly comparison due to data aggregation. The bias revealed that GPM-IMERG07 and PERSIANN-CDR underestimated and overestimated precipitation in daily and monthly comparisons, respectively, while the vice versa was for CHIRPS2.0 and CPC-CMORPH. In addition, the findings revealed that PERSIAN-CDR and GPM-IMERG07 agreed better with the ground observations, whereas PERSIANN-CDR had the lowest RMSE and better bias values compared to other SPPs at daily and monthly temporal resolutions. In the case of categorical statistics, PERSIANN-CDR demonstrated better daily rainfall detection capability than CHIRPS2.0, CPC-CMORPH, and GPM-IMERG07. The performance analysis of SPPs appears to be best when the frequency of "miss" rainfall events and the magnitude of "miss-bias" rainfall are the lowest. This is because "miss" events directly reflect the satellite algorithm's sensitivity to rainfall detection, while "miss-bias" quantifies this sensitivity. PERSIANN-CDR had the lowest miss bias compared to other SPPs in the case of 4CED. However, it can be deduced from this study that precipitation estimates from SPPs may require additional processes before applying in hydrological studies because of the magnitude of their inherent biases. The study recommends that the algorithm developer improve the precipitation retrieval algorithm by reducing biases in the SPPs. In addition, end users are encouraged to perform bias correction or data merging to boost the accuracy of the rainfall estimates for improved hydrological simulations, weather forecasting, climate monitoring, and other environment-related studies.

Acknowledgements This work is part of the research funded by the Tertiary Education Trusted Fund (TETFUND), Nigeria under the Overseas PhD scholarship scheme. The authors also appreciate the financial support provided by the Ministry of Higher Education, Malaysia via the FRGS grant (Grant number: FRGS/1/2020/TK0/UM/02/19) and the Presidents' Forum of Southeast Asia and Taiwan Universities via the SATU Joint Research Scheme (ST004-2024). We would like to thank the Nigerian Meteorological Agency (NiMET) for making the ground observations available.

Author contributions All authors contributed to the study's conception and design. Material preparation, data collection and analysis were performed by Habeeb Oladimeji Ganiyu. The first draft of the manuscript was written by Habeeb Oladimeji Ganiyu and all authors commented on previous versions of the manuscript. All authors read and approved the final manuscript.

Funding This work is part of the research funded by the Tertiary Education Trusted Fund (TETFUND), Nigeria under the Overseas PhD scholarship scheme. The authors also appreciate the financial support provided by the Ministry of Higher Education, Malaysia, via the FRGS grant (Grant number: FRGS/1/2020/TK0/UM/02/19) and the UM International Collaboration Grant (SATU ST004-2024).

Data availability The ground observations used for this research article are available from the first author upon reasonable request. CHIRPS is available at https://data.chc.ucsb.edu/products/CHIRPS-2.0/global_daily/netcdf/, CPC-CMORPH is available at https://www.ncei.noaa.gov/data/cmorph-high-resolution-global-precipitation-estimates/access/daily/, GPM-IMERG Final version 7 is available at https://disc.gsfc.nasa.gov/datasets/GPM_3IMERGDF_07/summary?keywords=GPM_IMERG%20Final, and PERSIANN-CDR is available at https://www.ncei.noaa.gov/data/precipitation-persiann/access/.

Declarations

Competing interests The authors declare no competing interests.

References

Adedeji O, Olusola A, Babamaaji R, Adelabu S (2021) An assessment of flood events along lower niger using sentinel-1 imagery. Environ Monit Assess 193(12). https://doi.org/10.1007/s10661-021-09647-1

Adenodi RA, Akinnubi R, Ojo OL, Kolebaje OT, Akinyemi P (2016) Analysis of the coverage area of NiMET weather stations in Nigeria based on WMO standard. Niger J Space Res 14(1):1–4

Adjei KA, Ren L, Appiah-Adjei EK, Odai SN (2015) Application of satellite-derived rainfall for hydrological modelling in the data-scarce black volta trans-boundary basin. Hydrol Res 46(5):777–791. https://doi.org/10.2166/nh.2014.111

Akinyemi DF, Ayanlade OS, Nwaezeigwe JO, Ayanlade A (2020) A comparison of the accuracy of multi-satellite precipitation estimation and ground meteorological records over southwestern Nigeria. Remote Sens Earth Syst Sci 3:1–2. https://doi.org/10.1007/s41976-019-00029-3

Almagro A, Oliveira PTS, Brocca L (2021) Assessment of bottom-up satellite rainfall products on estimating river discharge

and hydrologic signatures in Brazilian catchments. J Hydrol 603:126897. https://doi.org/10.1016/j.jhydrol.2021.126897

Ayehu GT, Tadesse T, Gessesse B, Dinku T (2018) Validation of new satellite rainfall products over the Upper Blue Nile Basin, Ethiopia. Atmos Meas Tech 11(4):1921–1936. https://doi.org/10.5194/amt-11-1921-2018

Chen H, Yong B, Kirstetter PE, Wang L, Hong Y (2021) Global component analysis of errors in three satellite-only global precipitation estimates. Hydrol Earth Syst Sci 25(6):3087–3104. https://doi.org/10.5194/hess-25-3087-2021

Chen Z, Wen Z, Wu R, Zhao P, Cao J (2014) Influence of two types of El Niños on the east Asian climate during boreal summer: a numerical study. Clim Dyn 43(1–2):469–481. https://doi.org/10.1007/s00382-013-1943-1

Core Team R (2019) R: a language and environment for statistical computing. R Foundation Stat Comput Vienna Austria. https://doi.org/10.1108/eb003648

de Carvalho JW, Loireau M, Fargette F, Filho BC, Wélé A (2017) Correlation between soil erosion and satellite data on areas of current desertification: a case study in Senegal. Ciência E Tropic 41:51–66

Dembélé M, Zwart SJ (2016) Evaluation and comparison of satellite-based rainfall products in Burkina Faso, West Africa. Int J Remote Sens 37(17):3995–4014. https://doi.org/10.1080/01431161.2016.1207258

Dinku T, Funk C, Peterson P, Maidment R, Tadesse T, Gadain H, Ceccato P (2018) Validation of the CHIRPS satellite rainfall estimates over eastern Africa. Q J R Meteorol Soc 144:292–312. https://doi.org/10.1002/qj.3244

Dinku T, Hailemariam K, Maidment R, Tarnavsky E, Connor S (2014) Combined use of satellite estimates and rain gauge observations to generate high-quality historical rainfall time series over Ethiopia. Int J Climatol 34(7):2489–2504. https://doi.org/10.1002/joc.3855

Fasipe OA, Izinyon OC (2021) Exponent determination in a poorly gauged basin system in Nigeria based on flow characteristics investigation and regionalization method. SN Appl Sci 3(3). https://doi.org/10.1007/s42452-021-04302-3

Funk C, Peterson P, Landsfeld M, Pedreros D, Verdin J, Shukla S, Husak G, Rowland J, Harrison L, Hoell A, Michaelsen J (2015) The climate hazards infrared precipitation with stations - a new environmental record for monitoring extremes. Sci Data 2. https://doi.org/10.1038/sdata.2015.66

Gebregiorgis AS, Kirstetter PE, Hong YE, Gourley JJ, Huffman GJ, Petersen WA, Xue X, Schwaller MR (2018) To what extent is the day 1 GPM IMERG satellite precipitation estimate improved as compared to TRMM TMPA-RT? J Geophys Research: Atmos 123(3):1694–1707. https://doi.org/10.1002/2017JD027606

Gebremedhin MA, Lubczynski MW, Maathuis BHP, Teka D (2021) Novel approach to integrate daily satellite rainfall with in-situ rainfall, Upper Tekeze Basin, Ethiopia. Atmos Res 248:105135. https://doi.org/10.1016/j.atmosres.2020.105135

Goshime DW, Absi R, Ledésert B (2019) Evaluation and bias correction of CHIRP rainfall estimate for rainfall-runoff simulation over Lake Ziway Watershed, Ethiopia. Hydrology 6(3). https://doi.org/10.3390/hydrology6030068

Gunathilake MB, Amaratunga YV, Perera A, Karunanayake C, Gunathilake AS, Rathnayake U (2020) Statistical evaluation and hydrologic simulation capacity of different satellite-based precipitation products (SbPPs) in the Upper Nan River Basin, Northern Thailand. J Hydrology: Reg Stud 32:100743. https://doi.org/10.1016/j.ejrh.2020.100743

Haile AT, Tefera FT, Rientjes T (2016) Flood forecasting in Niger-Benue basin using satellite and quantitative precipitation forecast data. Int J Appl Earth Obs Geoinf 52:475–484. https://doi.org/10.1016/j.jag.2016.06.021

Helmi AM, Abdelhamed MS (2023) Evaluation of CMORPH, PERSIANN-CDR, CHIRPS V2.0, TMPA 3B42 V7, and GPM IMERG V6 Satellite Precipitation Datasets in Arabian Arid Regions. Water (Switzerland) 15(1):92. https://doi.org/10.3390/w15010092

Hsu KL, Gao X, Sorooshian S, Gupta HV (1997) Precipitation estimation from remotely sensed information using artificial neural networks. J Appl Meteorol 36:1176–1190

Huffman GJ, Adler RF, Bolvin DT, Gu G, Nelkin EJ, Bowman KP, Hong Y, Stocker EF, Wolff DB (2007) The TRMM Multisatellite Precipitation Analysis (TMPA): quasi-global, multiyear, combined-sensor precipitation estimates at fine scales. J Hydrometeorol 8(1):38–55. https://doi.org/10.1175/JHM560.1

Huffman GJ, Bolvin DT, Braithwaite D, Hsu K, Joyce R, Kidd C et al (2019) NASA global precipitation measurement (GPM) integrated multi-satellitE retrievals for GPM (IMERG) algorithm theoretical basis document (ATBD) version 6.0 (p 14). Retrieved from https://pps.gsfc.nasa.gov/Documents/IMERG_ATBD_V15.11.pdf. Accessed 20 Sept 2023

Huffman GJ, Bolvin DT, Joyce R, Nelkin EJ, Tan J, Braithwaite D, Hsu K, Kelley OA, Nguyen P, Sorooshian S, Watters DC, West BJ, Xie P (2023) Algorithm Theoretical Basis Document (ATBD) NASA Global Precipitation Measurement (GPM) Integrated Multi-satellitE Retrievals for GPM (IMERG) Version 07. Retrieved from https://disc.gsfc.nasa.gov/datasets/GPM_3IMERGDF_07/summary_keywords=GPM_IMERG%20Final. Accessed 25 Oct 2023

Hussain S, Song X, Ren G, Hussain I, Han D, Zaman MH (2017) Evaluation of gridded precipitation data in the Hindu Kush–Karakoram–Himalaya mountainous area. Hydrol Sci J 62(14):2393–2405. https://doi.org/10.1080/02626667.2017.1384548

Hussain Y, Satgé F, Babar Hussain M, Martinez-Carvajal H, Bonnet M-P, Cárdenas-Soto M, Llacer Roig H, Akhter G (2017) Performance of CMORPH, TMPA, and PERSIANN rainfall datasets over plain, mountainous, and glacial regions of Pakistan. Theoret Appl Climatol 131(4):1119–1132

Ji H, Peng D, Gu Y, Liang Y, Luo X (2022) Evaluation of multiple satellite precipitation products and their potential utilities in the Yarlung Zangbo River Basin. Sci Rep 12(1). https://doi.org/10.1038/s41598-022-17551-y

Joyce RJ, Janowiak JE, Arkin PA, Xie P (2004) CMORPH: A method that produces global precipitation estimates from passive microwave and infrared data at high spatial and temporal resolution. J Hydrometeorol 15(3). https://doi.org/10.1175/1525-7541(2004)005%3C0487:CAMTPG%3E2.0.CO;2

Kabite Wedajo G, Kebede Muleta M, Gessesse Awoke B (2021) Performance evaluation of multiple satellite rainfall products for Dhidhessa River Basin (DRB), Ethiopia. Atmos Meas Tech 14(3):2299–2316. https://doi.org/10.5194/amt-14-2299-2021

Khan S, Khan F, Guan Y (2022) Assessment of gridded precipitation products in the hydrological modeling of a flood-prone mesoscale basin. Hydrol Res 53(1):85–106. https://doi.org/10.2166/NH.2021.073

Le AM, Pricope NG (2017) Increasing the accuracy of runoffand streamflow simulation in the Nzoia Basin, Western Kenya, through the incorporation of satellite-derived CHIRPS data. Water (Switzerland) 9(2):114. https://doi.org/10.3390/w9020114

Lekula M, Lubczynski MW, Shemang EM, Verhoef W (2018) Validation of satellite-based rainfall in Kalahari. Phys Chem Earth 105:84–97. https://doi.org/10.1016/j.pce.2018.02.010

Li Y, Zhang K, Bardossy A, Shen X, Cheng Y (2023) Evaluation and error decomposition of IMERG product based on multiple satellite sensors. Remote Sens 15(6):1710. https://doi.org/10.3390/rs15061710

Maidment RI, Grimes D, Black E, Tarnavsky E, Young M, Greatrex H, Allan RP, Stein T, Nkonde E, Senkunda S, Alcántara EMU (2017) A new, long-term daily satellite-based rainfall dataset for operational monitoring in Africa. Sci Data 4:170063. https://doi.org/10.1038/sdata.2017.63

Mianabadi A (2023) Evaluation of long-term satellite-based precipitation products for developing intensity-frequency (IF) curves of daily precipitation. Atmos Res 286. https://doi.org/10.1016/j.atmosres.2023.106667

Min X, Yang C, Dong N (2020) Merging satellite and gauge rainfalls for flood forecasting of two catchments under different climate conditions. Water (Switzerland) 12(3):802. https://doi.org/10.3390/w12030802

Moges DM, Kmoch A, Uuemaa E (2022) Application of satellite and reanalysis precipitation products for hydrological modeling in the data-scarce Porijõgi catchment. Estonia J Hydrology: Reg Stud 41:101070. https://doi.org/10.1016/j.ejrh.2022.101070

Ngene BU, Obianigwe N (2018) Nigerian rain gauge station optimization and national development: the importance of headcount. IOP Conf Series: Mater Sci Eng 413:413 012022 (**pdf (iop.org)**)

NIHSA (2022) Nigerian Hydrological Services Agency. Annual flood outlook publication. https://nihsa.gov.ng/publications/. Accessed 13 Feb 2023

Nwachukwu P, Satgé F, Yacoubi SE, Pinel S, Bonnet M (2020) From TRMM to GPM: how reliable are satellite-based precipitation data across Nigeria? Remote Sens 12(23):3964. https://doi.org/10.3390/RS12233964

Ogbu KN, Hounguè NR, Gbode IE, Tischbein B (2020) Performance evaluation of satellite-based rainfall products over Nigeria. Climate 8(10):1–23. https://doi.org/10.3390/cli8100103

Otache MY, Tyabo MA, Animashaun IM, Ezekiel LP (2016) Application of parametric-based framework for regionalisation of flow duration curves. J Geoscience Environ Prot 04(05):89–99. https://doi.org/10.4236/gep.2016.45009

Peng J, Liu T, Huang Y, Ling Y, Li Z, Bao A, Chen X, Kurban A, De Maeyer P (2021) Satellite-based precipitation datasets evaluation using gauge observation and hydrological modeling in a typical arid land watershed of central Asia. Remote Sens 13(2):1–26. https://doi.org/10.3390/rs13020221

Pereira DR, Oliveira AR, Costa MS, Ramos TB, Rollnic M, Neves RJJ (2024) Evaluation of precipitation products in a Brazilian watershed: Tocantins-Araguaia watershed case study. Theor Appl Climatol. https://doi.org/10.1007/s00704-024-05091-6

Poméon T, Jackisch D, Diekkrüger B (2017) Evaluating the performance of remotely sensed and reanalyzed precipitation data over West Africa using HBV light. J Hydrol 547:222–235. https://doi.org/10.1016/j.jhydrol.2017.01.055

QGIS Team (2019) QGIS geographic information system. Open-source geospatial foundation project. http://qgis.osgeo.org

Qin Y, Chen Z, Shen Y, Zhang S, Shi R (2014) Evaluation of satellite rainfall estimates over the Chinese mainland. Remote Sens 6(11):11649–11672. https://doi.org/10.3390/rs61111649

Rahmawati N, Lubczynski MW (2018) Validation of satellite daily rainfall estimates in complex terrain of Bali Island, Indonesia. Theoret Appl Climatol 134(1–2):513–532. https://doi.org/10.1007/s00704-017-2290-7

RStudio T (2019) RStudio: integrated development for R. RStudio, Inc., Boston, MA

Salami A, Fenta AA (2022) Spatio-temporal evaluation of open access precipitation products with rain gauge observations in Nigeria. Arab J Geosci 15(1785):1–20

Seyam M, Othman F (2015) Long-term variation analysis of a tropical river's annual streamflow regime over a 50-year period. Theoret Appl Climatol 121(1–2):71–85. https://doi.org/10.1007/s00704-014-1225-9

Sun Q, Miao C, Duan Q, Ashouri H, Sorooshian S, Hsu KL (2018) A review of global precipitation data sets: data sources, estimation, and intercomparisons. Rev Geophys 56(1):79–107. https://doi.org/10.1002/2017RG000574

Suri A, Azad S (2024) Optimal placement of rain gauge networks in complex terrains for monitoring extreme rainfall events: a review. Theoret Appl Climatol 155:2511–2521. https://doi.org/10.1007/s00704-024-04856-3

Thiemig V, Rojas R, Zambrano-Bigiarini M, Levizzani V, De Roo A (2012) Validation of satellite-based precipitation products over sparsely gauged African River basins. J Hydrometeorol 13(6):1760–1783. https://doi.org/10.1175/JHM-D-12-032.1

Touma D, Martinez C (2023) National center for atmospheric research staff the climate data guide: CHIRPS: Climate Hazards InfraRed Precipitation with Station data (version 2). Retrieved from https://climatedataguide.ucar.edu/climate-data/chirps-climate-hazards-infrared-precipitation-station-data-version-2 on 15/12/2024

Usman M, Ndehedehe CE, Ahmad B, Manzanas R, Adeyeri OE (2022) Modeling streamflow using multiple precipitation products in a topographically complex catchment. Model Earth Syst Environ 8(2):1875–1885. https://doi.org/10.1007/s40808-021-01198-1

Usman M, Nichol JE, Ibrahim AT, Buba LF (2018) A spatio-temporal analysis of trends in rainfall from long-term satellite rainfall products in the Sudano Sahelian zone of Nigeria. Agric for Meteorol 260–261:273–286. https://doi.org/10.1016/j.agrformet.2018.06.016

Uwe S (2018) CDO user guide uwe. Schulzweida-MPI for Meteorology. https://code.mpimet.mpg.de/projects/cdo/embedded/index.html

Vu TT, Li L, Jun KS (2018) Evaluation of multi-satellite precipitation products for streamflow simulations: A case study for the Han River Basin in the Korean Peninsula, East Asia. Water (Switzerland) 10(5):642. https://doi.org/10.3390/w10050642

Wang XL, Chen H, Wu Y, Feng Y, Pu Q (2010) New techniques for the detection and adjustment of shifts in daily precipitation data series. J Appl Meteorol Climatol 49(12):2416–2436. https://doi.org/10.1175/2010JAMC2376.1

Worqlul AW, Yen H, Collick AS, Tilahun SA, Langan S, Steenhuis TS (2017) Evaluation of CFSR, TMPA 3B42 and ground-based rainfall data as input for hydrological models, in data-scarce regions: the upper Blue Nile Basin, Ethiopia. CATENA 152:242–251. https://doi.org/10.1016/j.catena.2017.01.019

Yazdandoost F, Moradian S, Izadi A, Bavani AM (2020) A framework for developing a spatial high-resolution daily precipitation dataset over a data-sparse region. Heliyon 6(9). https://doi.org/10.1016/j.heliyon.2020.e05091

Yong B, Chen B, Tian Y, Yu Z, Hong Y (2016) Error-component analysis of TRMM-based Multi-Satellite Precipitation Estimates over mainland China. Remote Sens 8(5):440. https://doi.org/10.3390/rs8050440

Yuan F, Zhang L, Wah Win KW, Ren L, Zhao C, Zhu Y, Jiang S, Liu Y (2017) Assessment of GPM and TRMM multi-satellite precipitation products in streamflow simulations in a data sparse mountainous watershed in Myanmar. Remote Sens 9(3):302. https://doi.org/10.3390/rs9030302

Yue H, Gebremichael M, Nourani V (2022) Performance of the global forecast system's medium-range precipitation forecasts in the Niger River basin using multiple satellite-based products. Hydrol Earth Syst Sci 26(1):167–181. https://doi.org/10.5194/hess-26-167-2022

Zhang Y, Ye A, Nguyen P, Analui B, Sorooshian S, Hsu K (2021) New insights into error decomposition for precipitation products. Geophys Res Lett 48(17):e2021GL094092. https://doi.org/10.1029/2021GL094092

Publisher's Note Springer Nature remains neutral with regard to jurisdictional claims in published maps and institutional affiliations.

Springer Nature or its licensor (e.g. a society or other partner) holds exclusive rights to this article under a publishing agreement with the author(s) or other rightsholder(s); author self-archiving of the accepted manuscript version of this article is solely governed by the terms of such publishing agreement and applicable law.